Effects of simulated secondary organic aerosol water on fine PM levels and composition over US

Stylianos Kakavas[1,2], Spyros N. Pandis[1,2] and Athanasios Nenes[1,3]

[1]Institute of Chemical Engineering Sciences, Foundation for Research and Technology Hellas, Patras, Greece

[2]Department of Chemical Engineering, University of Patras, Patras, Greece

[3]School of Architecture, Civil and Environmental Engineering, École Polytechnique Fédérale de Lausanne (EPFL), Switzerland

Correspondence to: Spyros N. Pandis (spyros@chemeng.upatras.gr) and Athanasios Nenes (athanasios.nenes@epfl.ch).

Abstract. Water is a key component of atmospheric aerosol, affecting many aerosol processes including gas/particle partitioning of semi-volatile compounds. Water related to secondary organic aerosol (SOAW) is often neglected in atmospheric chemical transport models and is not considered in gas-to-particle partitioning calculations for inorganic species. We use a new inorganic aerosol thermodynamics model, ISORROPIA-lite, which considers the effects of SOAW, to perform chemical transport model simulations for a year over the continental United States to quantify its effects on aerosol mass concentration and composition. SOAW can increase average fine aerosol water levels up to a factor of two when secondary organic aerosol (SOA) is a major PM_1 component. This is often the case in the south-eastern U.S where SOA concentrations are higher. Although the annual average impact of this added water on total dry PM_1 concentrations due to increased partitioning of nitrate and ammonium is small (up to 0.1 μg m^{-3}), total dry PM_1 increases of up to 2 μg m^{-3} (with nitrate levels increases up to 200%) can occur when RH levels and PM_1 concentrations are high.

1. Introduction

Atmospheric particulate matter with aerodynamic diameter smaller than 1 μm (PM_1) has adverse effects on public health, climate and ecosystem productivity (Pye et al., 2020; Baker et al., 2021; Guo et al., 2021). PM_1 is composed of thousands of organic compounds, black carbon (BC), and inorganic components such as sulfate (SO_4^{2-}),

nitrate (NO_3^-), ammonium (NH_4^+) and chloride (Cl^-) (Seinfeld and Pandis, 2006). Ambient aerosol is mostly composed of water which is determined by the chemical equilibrium of water vapor with the aerosol constituents (Liao and Seinfeld, 2005; Carlton and Turpin, 2013; Bian et al., 2014; Guo et al., 2015; Bougiatioti et al., 2016; Nguyen et al., 2016; Guo et al., 2017; Deetz et al., 2018; Kuang et al., 2018; Song et al., 2018; Wu et al., 2018; Pye et al., 2020; Gopinath et al., 2022). Aerosol liquid water directly affects the PM sensitivity and dry deposition rates, with direct implications for emissions control policy (Nenes et al., 2020; Nenes et al., 2021; Sun et al., 2021).

The hygroscopicity parameter (κ), which expresses the ability of a PM component to absorb water, is an effective approach for the parameterization of the water uptake of atmospheric PM that is a mixture of organic and inorganic species (Petters and Kreidenweis, 2007). Although organic aerosol (OA) is less hygroscopic than inorganic salts, it can still contribute significantly to the total aerosol water (Guo et al., 2015; Bougiatioti et al., 2016; Jathar et al., 2016; Li et al., 2019) or can even become the dominant contributor at lower ambient relative humidity (Jin et al., 2020). Previous studies have demonstrated that secondary organic aerosol (SOA) is a lot more hygroscopic ($0.1 \leq \kappa \leq 0.3$) than primary organic aerosol (POA) ($\kappa \leq 0.01$) and is mainly responsible for the corresponding OA water (Petters et al., 2006; Koehler et al., 2009; Chang et al., 2010; Jathar et al., 2016; Kuang et al., 2020; Li et al., 2020).

SOAW can enhance secondary inorganic aerosol concentrations assisting in their partitioning in the particulate phase to satisfy equilibrium. However, such effects are not considered in thermodynamic modules used for the simulation of gas-to-particle partitioning of inorganic species in chemical transport models. Evidence exists however that fine aerosol nitrate and ammonium concentrations can increase in areas with high organic aerosol and RH levels (Kakavas et al., 2022). The importance of these SOAW impacts on secondary aerosol formations has not been systematically studied and is the focus of this work.

We use a new aerosol thermodynamics model, ISORROPIA-lite (Kakavas et al., 2022), to simulate SOAW effects on the partitioning of the inorganic components, for a year over the continental United States. The model performance has been evaluated for fine PM and its components for the examined period by Skyllakou et al. (2021). Its predictions were compared against $PM_{2.5}$ composition measurements from approximately 300 stations of the CSN and IMPROVE networks and $PM_{2.5}$ mass

concentrations from 1067 stations. The PMCAMx performance was found to be good for the total $PM_{2.5}$ concentration (fractional bias less than 30% and fractional error less than 50%) and average (fractional bias less than 60% and fractional error less than 75%) for its major components. Details about the evaluation can be found in Skyllakou et al. (2021). The aim of our work is to quantify the SOAW contribution to the total fine PM water and to study its effects on inorganic aerosol thermodynamics and total dry fine PM levels and composition.

2. Methods

2.1 ISORROPIA-lite

ISORROPIA-lite is a lean and accelerated version of the widely used ISORROPIA-II (Fountoukis and Nenes, 2007) aerosol thermodynamics model. It assumes that the aerosol exists only in the metastable state at low RH and the activity coefficients of ionic pairs are always obtained from precalculated look-up tables. It estimates aerosol water associated with each one of the aerosol components. Furthermore, ISORROPIA-lite has an important additional feature compared to ISORROPIA-II, as it considers the effects of SOAW on inorganic aerosol thermodynamics. The resulting increase of the total water mass drives more of the water-soluble gaseous species to the particle phase to satisfy equilibrium. SOAW, W_{SOA}, in ISORROPIA-lite is calculated using the well-established κ-Kohler theory of Petters and Kreidenweis (2007):

$$W_{SOA} = \frac{\rho_w}{\rho_{SOA}} \frac{C_{SOA}\kappa}{\left(\frac{1}{RH} - 1\right)} \quad (1)$$

where ρ_w is the density of water, ρ_{SOA} the SOA density, C_{SOA} the SOA concentration, κ the SOA hygroscopicity parameter and RH the relative humidity in the 0−1 scale. More details about the ISORROPIA-lite can be found in Kakavas et al. (2022).

2.2 PMCAMx description and application

PMCAMx (Karydis et al., 2010; Tsimpidi et al., 2010) is a three dimensional chemical transport model based on CAMx (Environ, 2006), which simulates horizontal and vertical advection and dispersion, dry and wet deposition, as well as aqueous, gas, and aerosol chemistry. The mechanism used in this work for gas-phase chemistry simulations is the Carbon Bond 05 (CB5) (Yarwood et al., 2005) and

includes 190 reactions of 79 gas species. To describe the aerosol size and composition distribution 10-size sections (from 40 nm to 40 μm) are used assuming that all particles in each size bin have the same composition. Therefore, PMCAMx predicts the PM_x concentration where x can be among other choices 1, 2.5 and 10 μm. Equilibrium is always assumed between the bulk aerosol and gas phases. The partitioning of semi-volatile inorganic species between the gas and particulate phases is simulated by ISORROPIA-lite. Weighting factors based on each size bin's effective surface area are used to distribute to the various size bins the mass transferred between the two phases in each time step (Pandis et al., 1993). For the simulation of organic aerosols, the volatility basis set approach (Donahue et al., 2006) is used. POA is simulated using eight volatility bins (from 10^{-1} to 10^{6} $\mu g\,m^{-3}$) at 298 K, while for SOA four volatility bins (1, 10, 10^2, 10^3 $\mu g\,m^{-3}$) at 298 K are used (Murphy and Pandis, 2009). For the major point sources, the NO_x plumes are simulated using the Plume-in-Grid (PiG) approach (Karamchandani et al., 2011; Zakoura and Pandis, 2019).

We applied PMCAMx over the continental United States during 2010. The modeling domain includes northern Mexico and southern Canada and covers a 4752 × 2952 km^2 region (Figure S1). The model grid consists of 10,824 cells with horizontal dimensions of 36 × 36 km. The meteorological inputs were provided by the Weather Research Forecasting model (WRF v3.6.1) using a horizontal resolution of 12 × 12 km. While it is difficult to measure accurately RH values above 95%, model predictions are more reliable. Therefore there was no need for screening of the few RH values above 95%. The gaseous and primary particle emissions were developed by Xing et al. (2013). More details about the meteorological inputs and the emissions can be found in Skyllakou et al. (2021).

To quantify the SOAW effects on inorganic aerosol thermodynamics three simulations were performed. The first was a simulation neglecting SOAW and including only inorganic aerosol water. Two additional simulations were performed: one where κ of SOA was assumed to be equal to 0.1 and one with κ=0.2 to examine how SOA hygroscopicity affects total fine aerosol water content and PM levels and composition. Previous studies have estimated secondary organic aerosol density values of 1−1.4 g cm^{-3} (Turpin and Lim, 2001; Kostenidou et al., 2007). A SOA density of 1 g cm^{-3} was assumed in the simulations. Higher densities suggest that

SOA particles may be in a solid or waxy state (Kostenidou et al., 2007). SOA exists mostly in submicrometer particles so our subsequent study focuses on PM_1.

3. Results

3.1 Effects of SOAW on PM_1 water levels

The annual average PM_1 water ground-level concentrations neglecting SOAW are shown in Figure 1. Higher PM_1 water concentrations from 8 to 18 μg m^{-3} are predicted in the north-eastern part of the US due to the higher inorganic PM_1 concentrations (Figure 2) and RH levels in that area. When SOAW is present in the simulations, total PM_1 water levels increase everywhere with higher fractional increases in the south-eastern US (up to 50% when κ=0.1 and up to 100% when κ=0.2 in Alabama and north-western Mexico) due to higher SOA levels (Figure S2). In the north-eastern US, lower fractional increases are predicted (10−15% when κ=0.1 and 20−30% when κ=0.2). In general, assuming a κ of SOA equal to 0.2 instead of 0.1 increases the corresponding amount of SOAW by about a factor of two. Figure 1 shows the distributions of fractional increase change in the annual PM_1 water levels at ground level from SOAW. Total PM_1 water average concentrations increase from 20 to 30% in about 60% of the modeling domain when κ=0.1. For κ=0.2, the corresponding increase is from 40 to 60%.

Predicted SOA levels are higher during summertime (Figure S2) since the emissions and oxidation rates of volatile organic compounds (VOCs) are higher (Zhang et al., 2013; Freney et al., 2014; Skyllakou et al., 2014; Fountoukis et al., 2016). However, even during wintertime fresh biomass burning emissions exposed to NO_2 and O_3 can form significant amounts of SOA in periods with low OH levels (Kodros et al., 2020). Higher total PM_1 water concentrations are predicted during winter (Figure 3) since the RH levels and inorganic fine aerosol concentrations are higher; especially nitrate and chloride which increasingly partition to the aerosol phase as temperature decreases (Guo et al., 2017). Predicted average PM_1 chloride concentrations are low (less than 0.1 μg m^{-3}) in all areas, with higher concentrations in parts of Kansas because of biomass burning in the simulated period. Higher fractional increases in fine aerosol water levels (up to 5 times) due to SOAW are predicted during summer in the south-eastern part of US where SOA concentrations are higher. This corresponds to increases to average fine aerosol water concentrations up to 8 μg m^{-3}.

Ammonium nitrate and ammonium sulfate are the inorganic salts that contribute the most to the total PM_1 water levels (Figure S3). SOAW also contributes significantly to the total PM_1 water levels especially in the south-eastern US (about 30 and 50% of total PM_1 water when κ=0.1 and κ=0.2 respectively), when the mass fraction of SOA in dry PM_1 exceeds 30%.

3.2 Effects of SOAW on total dry PM_1 levels

Higher dry PM_1 concentrations are predicted for the eastern part of the US (up to 15 $\mu g\ m^{-3}$) in the base case (Figure 4). These dry PM_1 levels increase slightly up to 0.6% and 1.2% due to SOAW when κ=0.1 and κ=0.2 for SOA is assumed. The highest annual average fractional increase in total dry PM_1 levels is predicted in California (1% when κ=0.1 and 2% when κ=0.2). The probability density (Figure 4) indicates that in about 60% of the modeling domain total dry fine aerosol concentrations increase up to 0.3% when κ=0.1. For κ=0.2, the corresponding increase is from 0.4 to 2%. The areas of the highest PM_1 increase correspond to regions where aerosol pH tends to be relatively high (Pye et al., 2020). In these areas, nitric acid and ammonia can condense and increase aerosol mass because of the increase in water from the SOA. Because of this partitioning change, the predicted gas-phase concentrations of semi-volatile inorganic components decreased on average when SOAW was considered (Figure S4). SOAW had a negligible absolute impact on the small fine chloride concentrations in this period (Figure 2). However, in periods during which chloride salts and SOA contribute significantly to the total dry (e.g. during intense biomass burning periods), fine chloride concentrations could also change (Metzger et al., 2006; Fountoukis et al., 2009; Gunthe et al., 2021).

Skyllakou et al. (2021) found that PMCAMx had a small fractional bias (5%) and fractional error (25%) for the annual average $PM_{2.5}$ concentrations of 1067 measurement stations in the U.S. The performance for annual average OA was similar (fractional bias of 5% and a fractional error of 26%) in 306 stations. Given that the addition of SOAW to the model had a small effect on the dry fine PM mass (of the order of 1%) there was no noticeable change in the already very good performance of the model for dry fine PM. Therefore, the major change in the model predictions is on the aerosol water concentrations.

3.3 Effects of SOAW on PM_1 components

The annual average results indicate that SOAW mainly affects fine aerosol water levels. To better analyze the effects of SOAW we focus on the temporal evolution of the predicted levels of PM_1 components in four sites (Figure S1) with different characteristics (Table S1). We have chosen one city from the West, one from the South, one from Southeast and one from the Northeast. They are all in different environments with different major sources and climatological conditions. The presence of SOAW increased PM_1 water concentrations in all sites from 1% to almost an order of magnitude (Figure 5). However, these fractional increases most of the time correspond to PM_1 water concentration increases of a few μg m^{-3} (Figure 6) because they occur under low RH levels. During higher RH periods (80 to 100%), the PM_1 water levels are predicted to increase up to 100 μg m^{-3} (e.g. in Toronto).

Total dry PM_1 concentrations during most of the simulated period increase on average less than 1% in all sites (Figure 5) due to SOAW. There are periods, however, with higher fractional increases (up to 10%) and even small decreases (up to 5%) in total dry fine aerosol levels in the examined sites. The decreases can be explained because SOAW increases the size of particles and therefore their dry deposition rate (Nenes et al., 2020). Depending on SOA hygroscopicity, increases up to 1.5 μg m^{-3} for nitrate and 0.5 μg m^{-3} for ammonium are predicted (Figure 6). Fine nitrate increases of 10% were more frequent in the examined sites; however higher increases up to 200% are predicted during the simulated period (Figure 7). As expected, higher increases can occur more often with higher assumed SOA hygroscopicity.

4. Discussion and Conclusions

Aerosol liquid water has a profound impact on aerosol processes, chemical composition and their impacts. By including the effects of organic water on inorganics thermodynamic equilibrium we show that SOAW can substantially increase aerosol water levels, on an average up to 60% over the majority of the domain. As a consequence, total dry PM_1 levels can also increase but the changes are small (up to 2% on an annual average basis). Locally these effects can be much more significant during periods of high RH and SOA levels (fine nitrate fractional increases can be as high as 200%).

The effects vary with season. During summer, the RH is lower and SOA levels are higher leading to higher fractional increases in aerosol water (Figure 3) but lower

absolute mass changes. During summer the fractional increases in total dry fine aerosol concentrations are lower than in wintertime (Figure S5). Responsible for the total dry fine aerosol concentration increases are nitrate and ammonium (Figure 2). These compounds partition together (as deliquesced ammonium nitrate) to the particulate phase to satisfy equilibrium due to the additional water mass of SOA.

The increases in total dry PM_1 and fine aerosol water levels depend on SOA concentrations, hygroscopicity value, RH levels and the particle phase fractions of inorganic species. The SOAW effect on aerosol water is approximately proportional to the assumed hygroscopicity parameter κ. Given that our work investigates the potential significance of this effect we have chosen to provide the results of two simulations one with relatively low and one with relatively high hygroscopicity of SOA. A more detailed treatment of the hygroscopicity parameter (e.g., assigning a different value to each OA component) will be a topic of future work.

The present work, thoroughly analyzes organic water uptake impacts over one simulated year (not just one month as done in Kakavas et al., 2022) and in quite a different geographical area (US here versus Europe in Kakavas et al., 2022). There are significant differences, but also similarities in the predicted changes and effects of SOA water. Both studies indicate that SOAW can contribute significantly to the total PM_1 water and increase particulate nitrate especially in areas with high total nitrate concentrations. Given this, and the important role of SOAW for climate forcing, visibility and chemistry, its inclusion in future studies is highly recommended. ISORROPIA-lite provides a simple and computationally effective approach for the simulation of SOAW.

Code and Data Availability. The model code and data used in this study are available from the authors upon request (spyros@chemeng.upatras.gr and athanasios.nenes@epfl.ch).

Author Contributions. SK incorporated ISORROPIA-lite in PMCAMx, carried out the simulations, analyzed the results and wrote the manuscript. SN and AN conceived and led the study and helped in the writing of the manuscript.

Competing Interests. The authors declare no competing financial interest.

Acknowledgements. This work was supported by the project FORCeS funded from the European Union's Horizon 2020 research and innovation programme under grant agreement No 821205, and project PyroTRACH (ERC-2016-COG) funded from H2020-EU.1.1. - Excellent Science - European Research Council (ERC), project ID 726165.

References

Baker, A., Kanakidou, M., Nenes, A., Myriokefalitakis, S., Croot, P.L., Duce, A. D., Gao, Y., Guieu, C., Ito, A., Jickells, T. D., Mahowald, N. M., Middag, R., Perron, M. M. G., Sarin, M. M., Shelley, R., and Turner, D. R.: Changing atmospheric acidity as a modulator of nutrient deposition and ocean biogeochemistry, Sci. Adv., 7, doi: 10.1126/sciadv.abd8800, 2021.

Bian, Y. X., Zhao, C. S., Ma, N., Chen, J., and Xu, W. Y.: A study of aerosol liquid water content based on hygroscopicity measurements at high relative humidity in the North China Plain, Atmos. Chem. Phys., 14, 6417−6426, 2014.

Bougiatioti, A., Nikolaou, P., Stavroulas, I., Kouvarakis, G., Weber, R., Nenes, A., Kanakidou, M., and Mihalopoulos, N.: Particle water and pH in the eastern Mediterranean: source variability and implications for nutrient availability, Atmos. Chem. Phys., 16, 4579–4591, 2016.

Carlton, A. G. and Turpin, B. J.: Particle partitioning potential of organic compounds is highest in the Eastern US and driven by anthropogenic water, Atmos. Chem. Phys., 13, 10203–10214, 2013.

Chang, R. Y.-W., Slowik, J. G., Shantz, N. C., Vlasenko, A., Liggio, J., Sjostedt, S. J., Leaitch, W. R., and Abbatt, J. P. D.: The hygroscopicity parameter (κ) of ambient organic aerosol at a field site subject to biogenic and anthropogenic influences: relationship to degree of aerosol oxidation, Atmos. Chem. Phys., 10, 5047–5064, 2010.

Deetz, K., Vogel, H., Haslett, S., Knippertz, P., Coe, H., and Vogel, B.: Aerosol liquid water content in the moist southern West African monsoon layer and its radiative impact, Atmos. Chem. Phys., 18, 14271−14295, 2018.

Donahue, N. M., Robinson, A. L., Stanier, C. O., and Pandis, S. N.: Coupled partitioning, dilution, and chemical aging of semivolatile organics, Environ. Sci. Technol., 40, 2635–2643, 2006.Environ: Comprehensive Air Quality

Model with Extensions Version 4.40. Users Guide. ENVIRON Int. Corp., Novato, CA, http://www.camx.com, 2006.

Fountoukis, C. and Nenes, A.: ISORROPIA II: a computationally efficient thermodynamic equilibrium model for K^+-Ca^{2+}-Mg^{2+}-NH_4^+-Na^+-SO_4^{2-}-NO_3^--Cl^--H_2O aerosols, Atmos. Chem. Phys., 7, 4639−4659, 2007.

Fountoukis, C., Nenes, A., Sullivan, A., Weber, R., Van Reken, T., Fischer, M., Matías, E., Moya, M., Farmer, D., and Cohen, R. C.: Thermodynamic characterization of Mexico City aerosol during MILAGRO 2006, Atmos. Chem. Phys., 9, 2141–2156, 2009.

Fountoukis, C., Megaritis, A. G., Skyllakou, K., Charalampidis, P. E., Denier van der Gon, H. A. C., Crippa, M., Prévôt, A. S. H., Fachinger, F., Wiedensohler, A., Pilinis, C., and Pandis, S. N.: Simulating the formation of carbonaceous aerosol in a European Megacity (Paris) during the MEGAPOLI summer and winter campaigns, Atmos. Chem. Phys., 16, 3727–3741, 2016.

Freney, E. J., Sellegri, K., Canonaco, F., Colomb, A., Borbon, A., Michoud, V., Doussin, J.-F., Crumeyrolle, S., Amarouche, N., Pichon, J.-M., Bourianne, T., Gomes, L., Prevot, A. S. H., Beekmann, M., and Schwarzenböeck, A.: Characterizing the impact of urban emissions on regional aerosol particles: airborne measurements during the MEGAPOLI experiment, Atmos. Chem. Phys., 14, 1397–1412, 2014.

Gopinath, A. K., Raj, S. S., Kommula, S. M., Jose, C., Panda, U., Bishambu, Y., Ojha, N., Ravikrishna, R., Liu, P., and Gunthe, S. S.: Complex interplay between organic and secondary inorganic aerosols with ambient relative humidity implicates the aerosol liquid water content over India during wintertime, J. Geophys. Res., 127, e2021JD036430, 2022.

Gunthe, S. S., Liu, P., Panda, U., Raj, S. S., Sharma, A., Derbyshire, E., Reyes-Villegas E., Allan, J., Chen, Y., Wang, X., Song, S., Pöhlker, M. L., Shi, L., Wang, Y., Kommula, S. M., Liu, T., Ravikrishna, R., McFiggans, G., Mickey, L. J., Martin, S. T., Pöschl, U., Andreae, M. O., and Coe, H.: Enhanced aerosol particle growth sustained by high continental chlorine emission in India., Nat. Geosci., 14, 77–84, 2021.

Guo, H., Xu, L., Bougiatioti, A., Cerully, K. M., Capps, S. L., Hite Jr., J. R., Carlton, A. G., Lee, S.-H., Bergin, M. H., Ng, N. L., Nenes, A., and Weber, R. J.: Fine-

particle water and pH in the southeastern United States, Atmos. Chem. Phys. 15, 5211–5228, 2015.

Guo, H., Liu, J., Froyd, K. D., Roberts, J. M., Veres, P. R., Hayes, P. L., Jimenez, J. L., Nenes, A., and Weber, R. J.: Fine particle pH and gas–particle phase partitioning of inorganic species in Pasadena, California, during the 2010 CalNex campaign, Atmos. Chem. Phys., 17, 5703–5719, 2017.

Guo, H., Li, X., Li, W., Wu, J., Wang, S., and Wei, J.: Climatic modification effects on the association between PM_1 and lung cancer incidence in China, BMC public health, 21, 880, 2021.

Jathar, S.H., Mahmud, A., Barsanti, K.C., Asher, W. E., Pankow, J. F., and Kleeman M. J.: Water uptake by organic aerosol and its influence on gas/particle partitioning of secondary organic aerosol in the United States, Atmos. Environ., 129, 142–154, 2016.

Jin, X., Wang, Y., Li, Z., Zhang, F., Xu, W., Sun, Y., Fan, X., Chen, G., Wu, H., Ren, J., Wang, Q., and Cribb, M.: Significant contribution of organics to aerosol liquid water content in winter in Beijing, China, Atmos. Chem. Phys., 20, 901–914, 2020.

Kakavas, S., Pandis, S. N., and Nenes, A.: ISORROPIA-lite: A comprehensive atmospheric aerosol thermodynamics module for Earth System Models, Tellus B, 74, 1−23, 2022.

Karamchandani, P., Vijayaraghavan, K., and Yarwood, G.: Sub-grid scale plume modeling, Atmosphere, 2, 389–406, 2011.

Karydis, V. A., Tsimpidi, A. P., Fountoukis, C., Nenes, A., Zavala, M., Lei, W., Molina, L. T., and Pandis, S. N.: Simulating the fine and coarse inorganic particulate matter concentrations in a polluted megacity, Atmos. Environ., 44, 608–620, 2010.

Kodros, J. K., Papanastasiou, D. K., Paglione, M., Masiol, M., Squizzato, S., Florou, K., Skyllakou, K., Kaltsonoudis, C., Nenes, A., and Pandis, S. N.: Rapid Dark Aging of Biomass Burning as an Overlooked Source of Oxidized Organic Aerosol., Proc. Natl. Acad. Sci. U.S.A., 117, 33028−33033, 2020.

Koehler, K. A., Kreidenweis, S. M., DeMott, P. J., Petters, M. D., Prenni, A. J., and Carrico, C. M.: Hygroscopicity and cloud droplet activation of mineral dust aerosol, Geoph. Res. Let., 36, (8), 2009.

Kostenidou, E., Pathak, R. K., and Pandis, S. N.: An algorithm for the calculation of secondary organic aerosol density combining AMS and SMPS data, Aerosol Sci. Technol., 41, (11), 1002–1010, 2007.

Kuang, Y., Zhao, C. S., Zhao, G., Tao, J. C., Xu, W., Ma, N., and Bian, Y. X.: A novel method for calculating ambient aerosol liquid water content based on measurements of a humidified nephelometer system, Atmospheric Measurement Techniques, 11, 2967−2982, 2018.

Kuang, Y., Xu, W., Tao, J., Ma, N., Zhao, C., and Shao, M.: A review on laboratory studies and field measurements of atmospheric organic aerosol hygroscopicity and its parameterization based on oxidation levels, Current Pollution Reports, 10.1007/s40726-020-00164-2, 2020.

Li, X., Song, S., Zhou, W., Hao, J., Worsnop, D. R., and Jiang, J.: Interactions between aerosol organic components and liquid water content during haze episodes in Beijing, Atmos. Chem. Phys., 19, 12163−12174, 2019.

Li, J., Zhang, H., Ying, Q., Wu, Z., Zhang, Y., Wang, X., Li, X., Sun, Y., Hu, M., Zhang, Y., and Hu, J.: Impacts of water partitioning and polarity of organic compounds on secondary organic aerosol over eastern China, Atmos. Chem. Phys., 20, 7291–7306, 2020.

Liao, H. and Seinfeld, J. H.: Global impacts of gas-phase chemistry aerosol interactions on direct radiative forcing by anthropogenic aerosols and ozone, J. Geophys. Res., 110, D18208, 2005.

Metzger, S., Mihalopoulos, N., and Lelieveld, J.: Importance of mineral cations and organics in gas-aerosol partitioning of reactive nitrogen compounds: case study based on MINOS results., Atmos. Chem. Phys., 6, 2549–2567, 2006.

Murphy, B. N. and Pandis, S. N.: Exploring summertime organic aerosol formation in the Eastern United States using a regional-scale budget approach and ambient measurements, J. Geophys. Res., 115, D24216, 2010.

Nenes, A., Pandis, S. N., Weber, R. J., and Russell, A.: Aerosol pH and liquid water content determine when particulate matter is sensitive to ammonia and nitrate availability, Atmos. Chem. Phys., 20, 3249–3258, 2020.

Nenes, A., Pandis, S. N., Kanakidou, M., Russell, A. G., Song, S., Vasilakos, P., and Weber, R. J.: Aerosol acidity and liquid water content regulate the dry deposition of inorganic reactive nitrogen, Atmos. Chem. Phys., 21, 6023–6033, 2021.

Nguyen, T. K. V., Zhang, Q., Jimenez, J. L., Pike, M., and Carlton, A. G.: Liquid water: ubiquitous contributor to aerosol mass. Environ. Sci. Tech. Let., 3, 257–263, 2016.

Pandis, S. N., Wexler, A. S., and Seinfeld, J. H.: Secondary organic aerosol formation and transport – II. Predicting the ambient secondary organic aerosol size distribution, Atmos. Environ., 27, 2403–2416, 1993.

Petters, M. D., Prenni, A. J., Kreidenweis, S. M., DeMott, P. J., Matsunaga, A., Lim, Y. B., and Ziemann, P. J.: Chemical aging and the hydrophobic-to-hydrophilic conversion of carbonaceous aerosol, Geophys. Res. Lett., 33, L24806, 2006.

Petters, M. D. and Kreidenweis, S. M.: A single parameter representation of hygroscopic growth and cloud condensation nucleus activity, Atmos. Chem. Phys., 7, 1961–1971, 2007.

Pye, H. O. T., Nenes, A., Alexander, B., Ault, A. P., Barth, M. C., Clegg, S. L., Collett Jr, J. L., Fahey, K. M., Hennigan, C. J., Herrmann, H., Kanakidou, M., Kelly, J. T., Ku, I.-T., McNeill, V. F., Riemer, N., Schaefer, T., Shi, G., Tilgner, A., Walker, J. T., Wang, T., Weber, R., Xing, J., Zaveri, R. A., and Zuend, A.: The acidity of atmospheric particles and clouds, Atmos. Chem. Phys., 20, 4809–4888, 2020.

Seinfeld, J. H. and Pandis, S. N.: Atmospheric chemistry and physics: From air pollution to climate change, Wiley: New York, 2006.

Skyllakou, K., Murphy, B. N., Megaritis, A. G., Fountoukis, C., and Pandis, S. N.: Contributions of local and regional sources to fine PM in the megacity of Paris, Atmos. Chem. Phys., 14, 2343– 2352, 2014.

Skyllakou, K., Rivera, P. G., Dinkelacker, B., Karnezi, E., Kioutsioukis, I., Hernandez, C., Adams, P. J., and Pandis, S. N.: Changes in $PM_{2.5}$ concentrations and their sources in the US from 1990 to 2010, Atmos. Chem. Phys., 21, 17115–17132, 2021.

Song, S., Gao, M., Xu, W., Shao, J., Shi, G., Wang, S., Wang, Y., Sun, Y., and McElroy, M. B.: Fine-particle pH for Beijing winter haze as inferred from different thermodynamic equilibrium models, Atmos. Chem. Phys., 18, 7423–7438, 2018.

Sun, X., Ivey, C. E., Baker, K. R., Nenes, A., Lareau, N. P., and Holmes, H. A.: Confronting Uncertainties of Simulated Air Pollution Concentrations during

Persistent Cold Air Pool Events in the Salt Lake Valley, Utah., Environ. Sci. Technol., 55, 15072−15081, 2021.

Tsimpidi, A. P., Karydis, V. A., Zavala, M., Lei, W., Molina, L., Ulbrich, I. M., Jimenez, J. L., and Pandis, S. N.: Evaluation of the volatility basis-set approach for the simulation of organic aerosol formation in the Mexico City metropolitan area, Atmos. Chem. Phys., 10, 525–546, 2010.

Turpin, B. J. and Lim, H. J.: Species contributions to $PM_{2.5}$ mass concentrations: revisiting common assumptions for estimating organic mass, Aerosol Sci. Technol., 35, 602–610, 2001.

Wu, Z., Wang, Y., Tan, T., Zhu, Y., Li, M., Shang, D., Wang, H., Lu, K., Guo, S., Zeng, L., and Zhang, Y.: Aerosol liquid water driven by anthropogenic inorganic salts: Implying its key role in haze formation over the North China Plain, Environ. Sci. & Tech. Letters, 10.1021/acs.estlett.8b00021, 2018.

Xing, J., Pleim, J., Mathur, R., Pouliot, G., Hogrefe, C., Gan, C.-M., and Wei, C.: Historical gaseous and primary aerosol emissions in the United States from 1990 to 2010, Atmos. Chem. Phys., 13, 7531–7549, 2013.

Yarwood, G., Rao, S., Yocke, M., and Whitten, G. Z.: Updates to the Carbon Bond Chemical Mechanism: CB05, Research Triangle Park, https://camx-wp.azurewebsites.net/Files/CB05_Final_Report_120805.pdf, 2005.

Zakoura, M. and Pandis, S. N.: Improving fine aerosol nitrate predictions using a Plume-in-Grid modeling approach, Atmos. Environ., 215, 116887, 2019.

Zhang, Q. J., Beekmann, M., Drewnick, F., Freutel, F., Schneider, J., Crippa, M., Prevot, A. S. H., Baltensperger, U., Poulain, L., Wiedensohler, A., Sciare, J., Gros, V., Borbon, A., Colomb, A., Michoud, V., Doussin, J.-F., Denier van der Gon, H. A. C., Haeffelin, M., Dupont, J.-C., Siour, G., Petetin, H., Bessagnet, B., Pandis, S. N., Hodzic, A., Sanchez, O., Honoré, C., and Perrussel, O.: Formation of organic aerosol in the Paris region during the MEGAPOLI summer campaign: evaluation of the volatility basis-set approach within the CHIMERE model, Atmos. Chem. Phys., 13, 5767–5790, 2013.

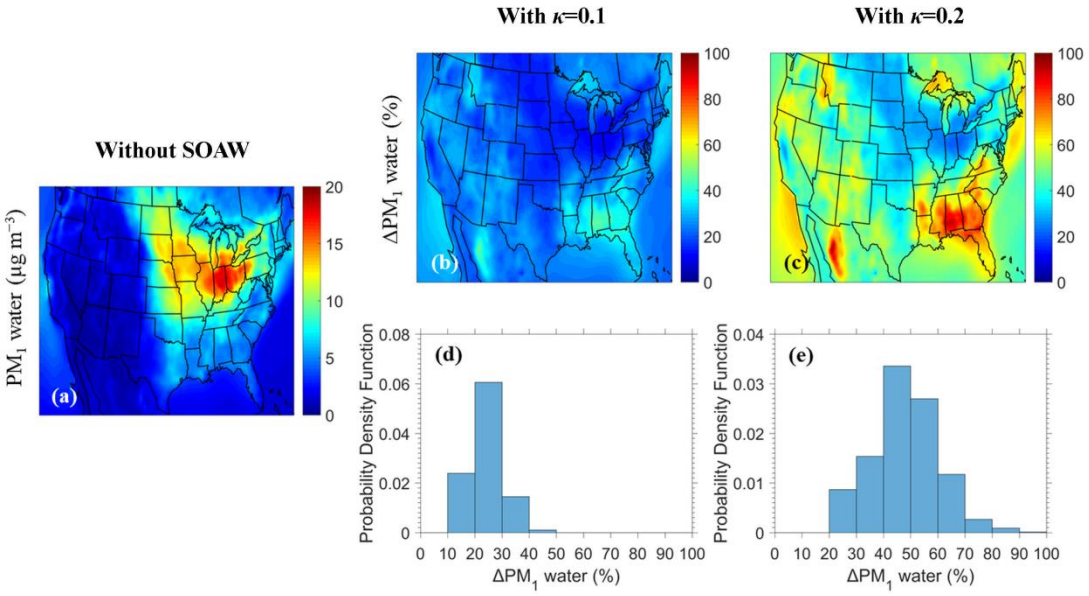

Figure 1. Maps of: **(a)** annual average PM_1 water ground-level concentrations neglecting SOAW, **(b)** annual average fractional increase of PM_1 water when SOAW is present in the simulations with κ=0.1 and, **(c)** with κ=0.2 during 2010. The probability density as a function of fractional increase in the annual PM_1 water concentrations due to SOAW when: **(d)** κ=0.1 and **(e)** κ=0.2 is shown.

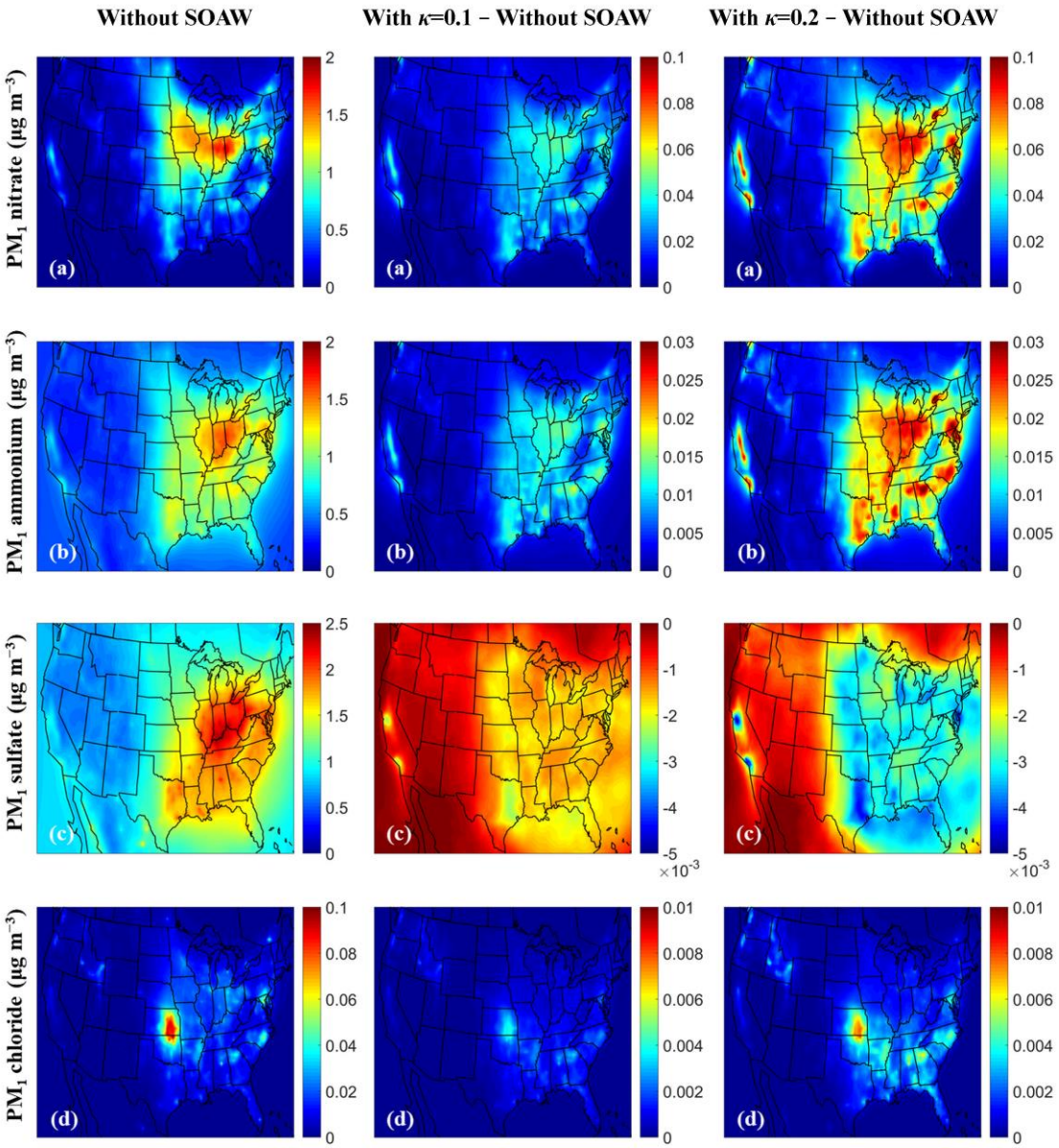

Figure 2. Annual average ground-level concentrations (in μg m^{-3}) of PM_1: **(a)** nitrate, **(b)** ammonium, **(c)** sulfate, and **(d)** chloride neglecting SOAW and the annual concentration changes when SOAW is present in the simulations with κ=0.1 and κ=0.2. A positive change corresponds to an increase. A negative change corresponds to a decrease.

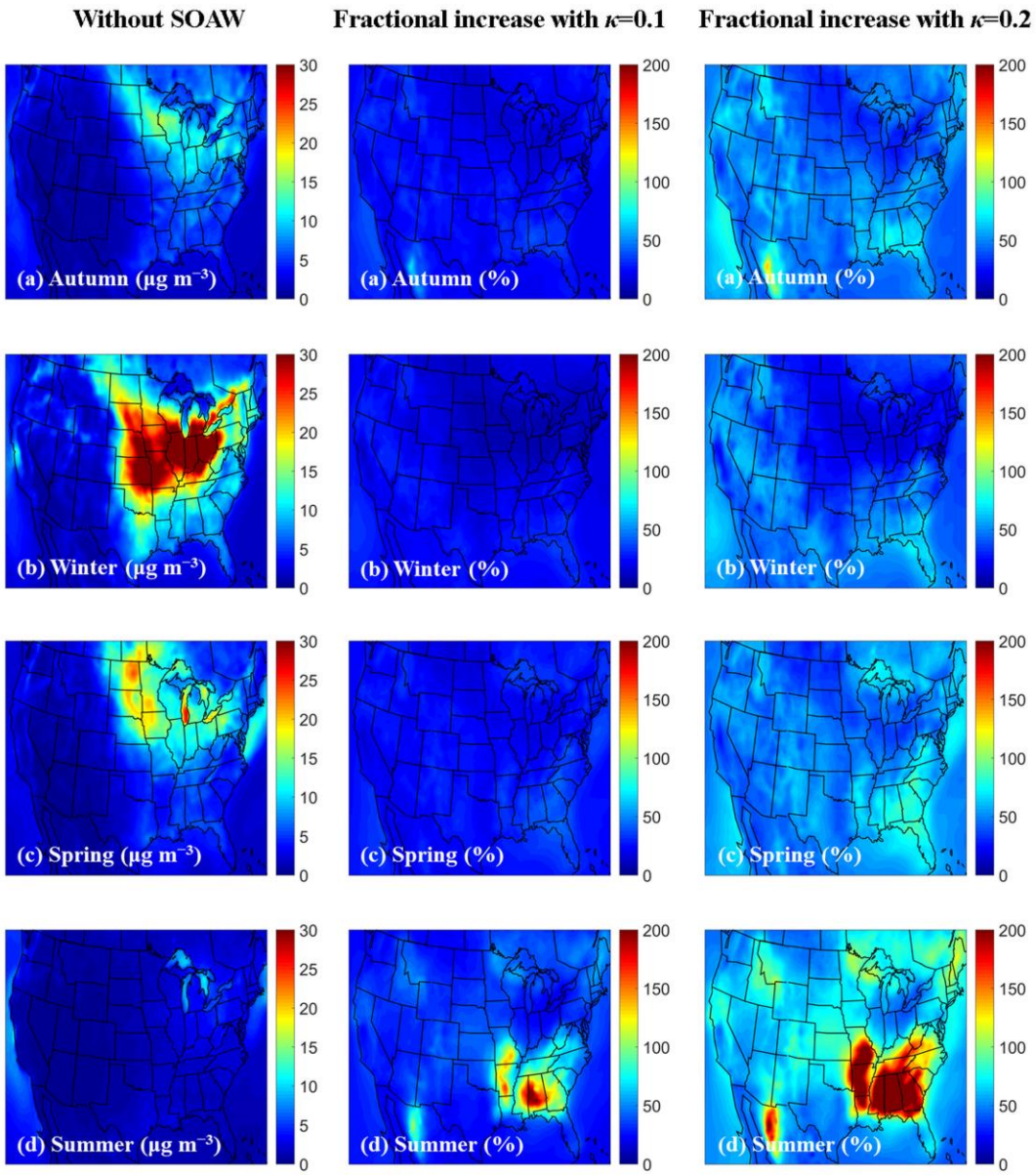

Figure 3. Average ground-level concentrations of PM_1 water neglecting SOAW (in μg m^{-3}) and the fractional increase when SOAW is present in the simulations with κ=0.1 and κ=0.2 during: **(a)** autumn (SON), **(b)** winter (DJF), **(c)** spring (MAM), and **(d)** summer (JJA) of 2010.

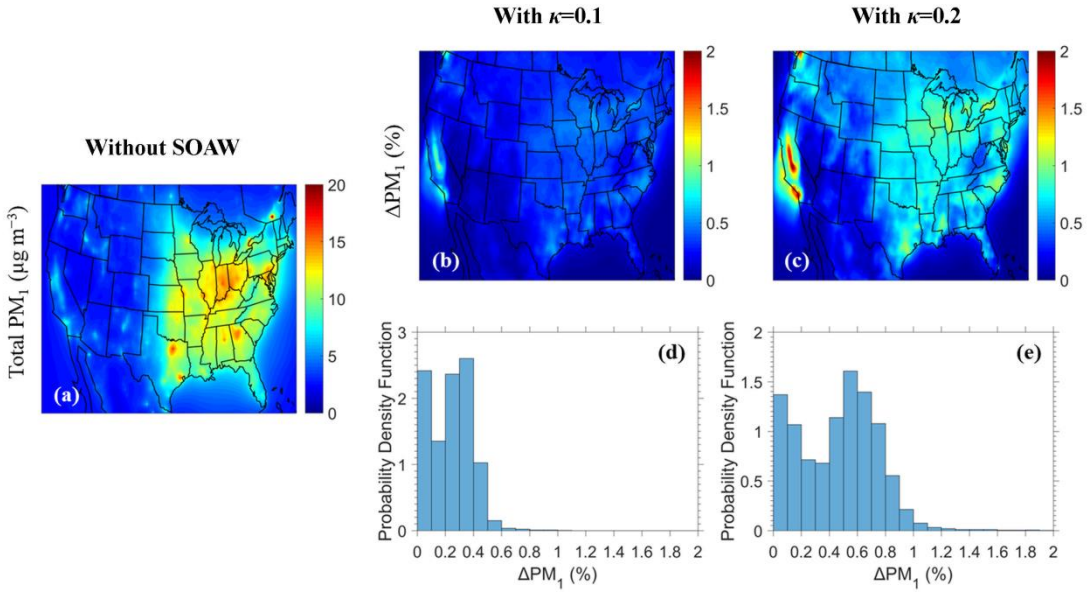

Figure 4. Maps of: **(a)** annual average total dry PM_1 ground-level concentrations neglecting SOAW, **(b)** annual average fractional increase of total dry PM_1 when SOAW is present in the simulations with κ=0.1 and, **(c)** with κ=0.2 during 2010. The probability density as a function of fractional increase in the annual total dry PM_1 concentrations due to SOAW when: **(d)** κ=0.1 and **(e)** κ=0.2 is shown.

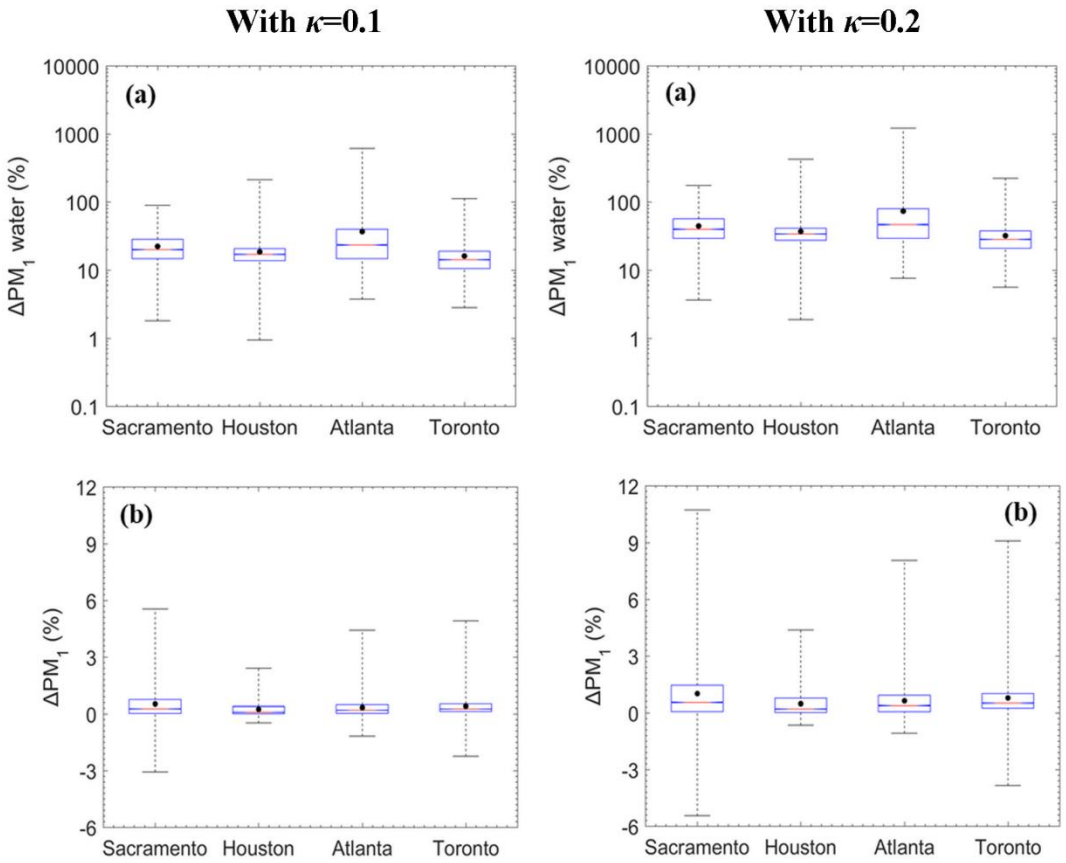

Figure 5. Box plots for fractional change in the hourly: **(a)** PM_1 water and **(b)** total dry PM_1 due to SOAW when κ=0.1 and κ=0.2 for Sacramento, California; Houston, Texas; Atlanta, Georgia; and Toronto, Canada during 2010. The red line represents the median, the black dot is the mean value, the upper box line is the upper quartile (75%) and the lower box line is the lower quartile (25%) of the distribution. A negative change corresponds to a decrease.

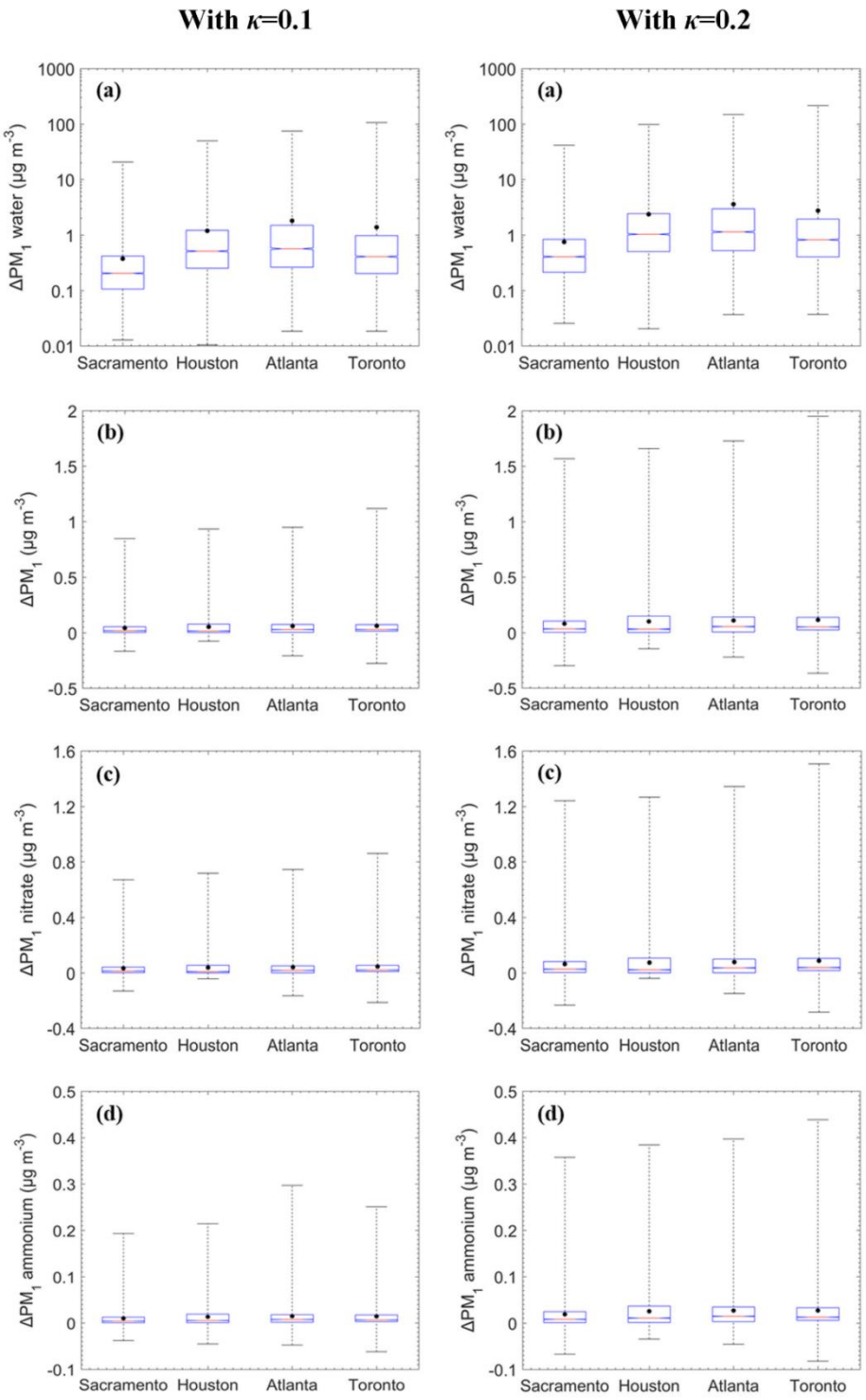

585

586

587 **Figure 6.** Box plots for concentration changes in the hourly PM_1: **(a)** water, **(b)** total
588 dry, **(c)** nitrate, and **(d)** ammonium due to SOAW when κ=0.1 and κ=0.2 for
589 Sacramento, California; Houston, Texas; Atlanta, Georgia; and Toronto, Canada
590 during 2010. The red line represents the median, the black dot is the mean value, the
591 upper box line is the upper quartile (75%) and the lower box line is the lower quartile
592 (25%) of the distribution. A negative change corresponds to a decrease. Water is in
593 log scale to show clearly both the relatively small average and the large range of high
594 values.

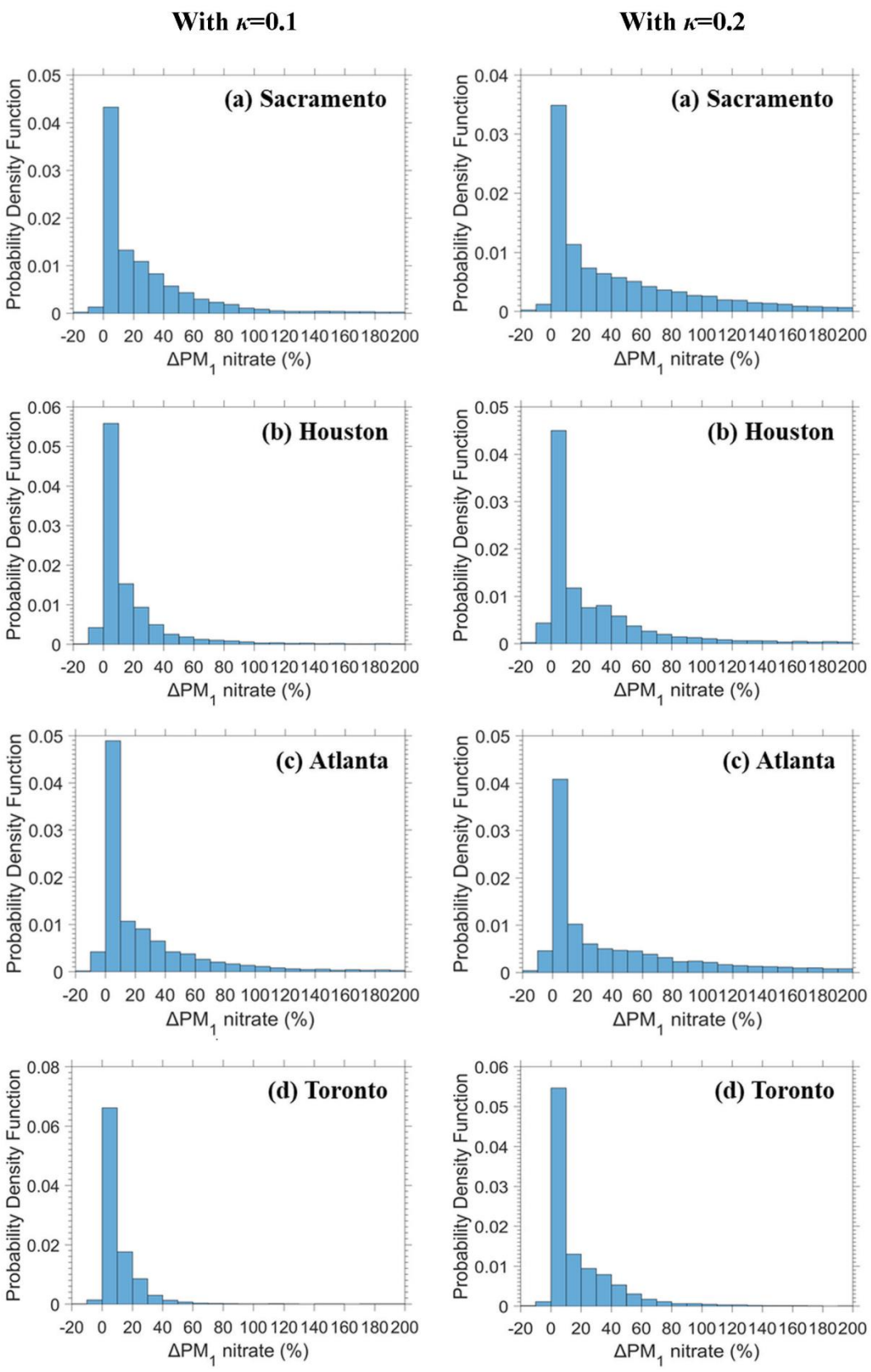

Figure 7. The probability density as a function of fractional increase in the hourly PM_1 nitrate due to SOAW when κ=0.1 and κ=0.2 for: **(a)** Sacramento, California; **(b)** Houston, Texas; **(c)** Atlanta, Georgia; and **(d)** Toronto, Canada during 2010.